Journal of Media, Culture and Communication
ISSN: 2799-1245
Vol: 04, No. 05, Aug-Sep 2024
http://journal.hmjournals.com/index.php/JMCC
DOI: https://doi.org/10.55529/jmcc.45.24.39

Characterization of Al-Substituted Ni-Zn Ferrites by XRD and FTIR Techniques

Mohammed Ghalib Ibrahim[1*], Abdulkarim Ziedan Khalf[2], Sabah M. Ali Ridha[3]

[1]Master student, Department of Physics,College of Education for Pure Sciences,University of Kirkuk, Kirkuk ,Iraq.*
[2]Lecturer doctor, Department of Physics, College of Education for Pure Sciences, University of Kirkuk, Kirkuk, Iraq.
[3]Professor, Department of Physics, College of Education for Pure Sciences, University of Kirkuk, Kirkuk, Iraq.

Email: [2]Karim_uok@uokirkuk.edu.iq, [3]Sabahyagmur@uokirkuk.edu.iq
Corresponding Email: [1]epsadmintsj@uokirkuk.edu.iq*

Received: 24 April 2024 **Accepted:** 10 July 2024 **Published:** 26 August 2024

Abstract*: *Ni0.5Zn0.5AlxFe2-xO4 (x = 0.00 to 0.50 in increments of 0.05) was prepared by the auto combustion sol-gel method, and the resulting nanopowder was subjected to calcination at three temperatures: 400, 600, and 800 °C. The structure of ferrite was characterized by XRD, and it was found that all the prepared Ni-Zn samples possess a single-phase cubic spinel structure, corresponding to the Fd-3m space group. The crystal lattice constant, a(Å), was calculated based on the resulting XRD patterns and it was found within the range of 8.312 to 8.386 Å, as the value of a(Å) decreases with increasing Al content, and increases with increasing temperature when the aluminum content (x) is constant. The Scherrer equation was used to calculate the crystalline size (D), with all samples in the range of 14.64 to 39.75 nm, and the crystalline size increases with increasing calcination temperature at a constant concentration, and increases with increasing aluminum content when the calcination temperature is constant. It was also found that the theoretical density, ρ_x, decreases with increasing aluminum content, and increases with increasing calcination temperature. The lengths of ionic jumps were calculated and it was found that the lengths of ionic jumps decrease with increasing Al content at a constant temperature. As FTIR spectroscopy analyzes showed the formation of Al-Ni-Zn Ferrite with a spinel structure, the increase in bond lengths in all samples leading to a decrease in the absorption frequency. The infrared absorption peaks become stronger and clearer, indicating an increase in the crystallinity of the samples, as the calcination temperature increases.

Keywords: Al-Ni-Zn Ferrite, XRD, Lattice Parameter, Crystallite Size, Theoretical Density, Hopping Length.

Journal of Media, Culture and Communication
ISSN: 2799-1245
Vol: 04, No. 05, Aug-Sep 2024
http://journal.hmjournals.com/index.php/JMCC
DOI: https://doi.org/10.55529/jmcc.45.24.39

1. INTRODUCTION

Spinel ferrites possess distinctive structural and magnetic properties, making them a focus of researchers in recent years. Its chemical stability, abundance in nature, high saturation magnetization, and high electrical resistance make it a suitable material as power transformers for use in electronic and communications applications. Since the structural, electrical and magnetic properties of spinel ferrite depend mainly on the manufacturing method, which causes a modification in the microstructure, the importance of the manufacturing method has emerged, as nickel and zinc ferrite were previously prepared using the traditional ceramic method, which requires high heat and long heating periods, which produces compounds with heterogeneous and undesirable crystal growth [1]. Due to the inability to control the method of crystal growth, the prepared ferrite has a large grain size and is not repeatable, which limits their applicability in advanced electronic and commucnication devices. Therefore, there is an urgent need to find a preparation method that guarantees the production of highly efficient materials with the required and desired properties. The most important of these methods are wet chemical methods such as auto combustion synthesis [2], co-precipitation [3], sol-gel [4] and others. The most important feature of these methods is the production of materials with nano-sized grains, providing a relatively large surface area, making them suitable for applications in electronic technology. Spinel ferrite has the chemical formula: AB_2O_4, where A and B are metal cations positioned in tetrahedral (A) and octahedral (B) sites, which can be classified into three types based on the occupancy proportions of these sites: normal ferrite, inverse ferrite, and random ferrite. In this research, aluminum-substituted nickel-zinc ferrite was prepared by the sol-gel auto combustion method at relatively low to moderate calcination temperatures to verify the potential to achieve superior electromagnetic properties at low calcination temperatures, which is considered a difficult challenge. This article highlights the role of aluminum substitution in the crystal structure of Zn-Ni ferrite and the effect of calcination temperature on the structural properties of nickel-zinc ferrite nanoparticles.

2. RELATED WORKS

[5] Characterized Ni-Zn ferrites substituted with Al using XRD and FTIR techniques. The study found that we have a coherent cubic spinel structure in all the prepared Ni-Zn samples, which corresponds to our present investigation. The results of this examination indicated that the lattice constant decreased with increasing amounts of Al and increased with increasing calcination temperature, which is consistent with our observations. [6] Conducted X-ray diffraction experiments, which show that lattice constant reduction is due to Aluminum introduction. This finding is consistent with our own observation of how Aluminium substitution affects the parameters of the lattice. [7] Used the XRD to determine the single phase cubic spinel structure and worked out the Scherrer equation, giving them crystallite sizes of 15-46 nm. The lattice constant of Ni decreased with increasing nickel ion concentration just as we found for Al substitution in our system. [8] Computed the average size of Nickel Zinc ferrite crystals from the Debye–Scherrer equation. Our study revealed similar trends in crystalline sizes at higher calcination temperatures as well as those related to increased aluminium contents as identified by this research paper. Additionally, it is discussed how one

Journal of Media, Culture and Communication
ISSN: 2799-1245
Vol: 04, No. 05, Aug-Sep 2024
http://journal.hmjournals.com/index.php/JMCC
DOI: https://doi.org/10.55529/jmcc.45.24.39

can analyze these ionic jump lengths and they relate to lattice parameters in brief which shows that ionic jump lengths decrease with increase in content of aluminium since aluminum ions are smaller than iron ions. This result confirms our findings about how dense is the crystal structure. [9] Adopted FTIR analysis to study the development of Al-Ni-
Zn ferrites which showed principal bands for metal-oxygen bonds. These imply that our FTIR spectroscopy agrees with a bond contraction model demonstrated through shifting absorption peaks towards lower wave numbers on increasing both Al content and calcination temperature. [10] Reported the alteration in absorption bands towards high frequencies at FTIR spectra of Ni-Zn ferrites substituted by Al. This shift correlates with a fall off of ionic radii that are changing bond lengths as well according to our results. [11] Also noted stronger and sharper infrared absorption peaks due to improved crystallinity at higher temperatures, which agrees with a correlation between higher calcination temperatures and more ordered cations as well as fewer structural distortions. [12] Also found a single-phase spinel structure with nanoparticle sizes through XRD for Ni0.7-xZn0.3MxFe2O4 where M = Mn 2+, Co 2+ and Cu 2+. In contrast, copper substitution did not affect the lattice constant but it increased when cobalt and manganese were used just like our observation that showed changes in lattice constant with respect to aluminium content.

3. METHODOLOGY

Experimental Details

Ni0.5Zn0.5AlxFe2-xO4 (x = 0.00 to 0.50 in increments of 0.05) was prepared by the sol-gel auto-combustion method, where iron (III) nitrate Fe $(NO_3)_3.9H_2O$, zinc nitrate Zn $(NO_3)_2 .6H_2O$, nickel nitrate Ni $(NO_3)_2 .6H_2O$, aluminum nitrate Al $(NO_3)_3 .9H_2O$, and citric acid $(C_6H_8O_7)$ were dissolved in deionized distilled water, and mixed using a magnetic stirrer for 30 minutes at room temperature until completely dissolved. An ammonia solution (NH_3) is added to adjust the pH to 7. A dark brown, blackish compound is produced. The temperature was gradually raised to 85°C over a period of three hours. The gases gradually evaporate, reducing volume and increasing viscosity until a gel state is reached, transitioning from solution to thick gel. When the temperature of the gel is raised to 200 °C, a swelling phenomenon occurs, which indicates the beginning of ignition. This combustion process continues until complete combustion is achieved. After burning, the gel undergoes transformation into a dry state, acquiring a dark brown to black color. Finally, the dried gel was lifted and subjected to fine grinding using a ceramic blender. The resulting powder is then placed in a ceramic crucible. It was then calcined using an electric oven at 400, 600, and 800 °C for three hours.

Chemical Name	Chemical formula	Mol. Mass (g.mol-1)	Purity %	Purpose	Supplier	Manufacturing company
Iron (III) Nitrate Nonahydrate	Fe (NO3)3.9H2O	404	98	Source of Fe cation	India	India

Journal of Media, Culture and Communication
ISSN: 2799-1245
Vol: 04, No. 05, Aug-Sep 2024
http://journal.hmjournals.com/index.php/JMCC
DOI: https://doi.org/10.55529/jmcc.45.24.39

Zinc Nitrate Hexahydrate	Zn (NO3)2 .6H 2O	297.48	98	Source of Zn cation	India	Sisco Researh Laboratories Pvt Ltd
Nickel Nitrate Hexahydrate	Ni(NO3)2 .6 H2O	290.79	97	Source of Ni cation	India	ACS Chemicals
Aluminum Nitrate Nonahydrate	Al (NO3)3 .9H 2O	40.00	98	Source of Al cation	India	Cynor Laboratorie
Ammonia solution	NH3	17.03	25	To adjust pH value of the solution	Belgium	Central Drug House (P) Ltd
Citric Acid	C6H8O7	192.13	99	Chelating agent	India	Loba Chemie Pvt. Ltd.

4. RESULTS AND DISCUSSIONS

XRD Characteristic

Fig. 1 (a) shows the XRD patterns indicate the presence of a single-phase cubic spinel structure, the sharp diffraction peaks show the good crystalline nature of the Al-Ni-Zn Ferrite samples, and the indexed levels of the as-prepared Al-Ni-Zn Ferrite spectrum agree with the diffraction levels listed under JCPDS Rule No. 08-0234 of the corresponding intense X-ray diffraction lines"(111), (220), (311), (222), (400), (422), (511), (440).), (620), (533), (622), and (444)", which correspond to the Fd-3m space group [9]. It was found that the ferrite phase appears clearly, and the intensity of the peaks increases with increasing temperature. It was also noted that the greatest intensity appears at the (311) plane for all samples, the dominant crystal orientation is at an angle 35.7°, corresponding to the peak (311), meaning this crystal orientation is the densest in the prepared zinc-nickel ferrite, meaning it is the crystal structure with a large uniform orientation at this peak, and it becomes clearer with increasing calcination temperature, which indicates that the compound becomes purer at the highest temperature (800 °C), and that the degree of crystallinity increases with increasing calcination temperature. This is evident from the decrease in FWHM with increasing temperature. These results are consistent with those of other researchers [10].

Journal of Media, Culture and Communication
ISSN: 2799-1245
Vol: 04, No. 05, Aug-Sep 2024
http://journal.hmjournals.com/index.php/JMCC
DOI: https://doi.org/10.55529/jmcc.45.24.39

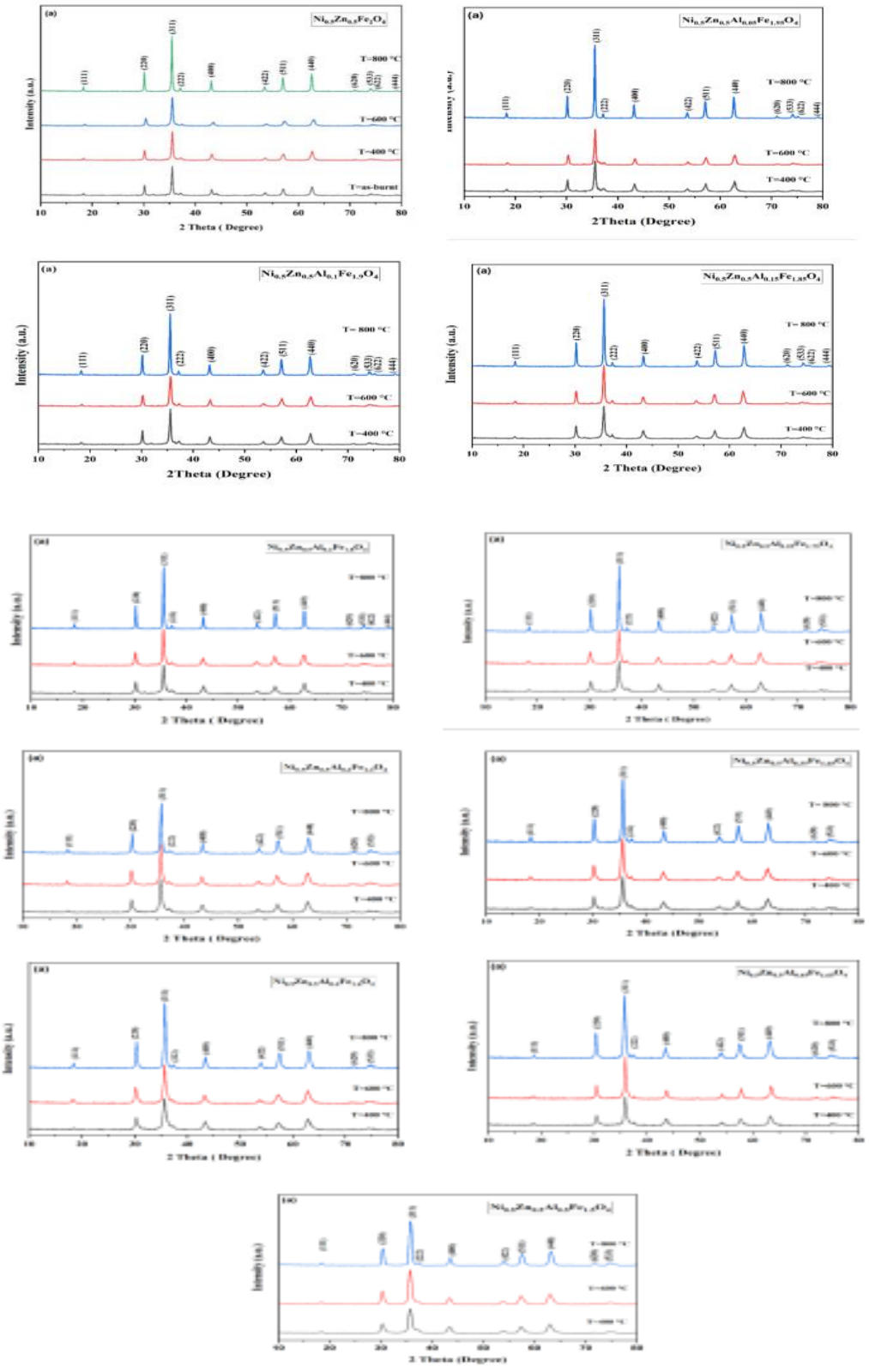

Journal of Media, Culture and Communication
ISSN: 2799-1245
Vol: 04, No. 05, Aug-Sep 2024
http://journal.hmjournals.com/index.php/JMCC
DOI: https://doi.org/10.55529/jmcc.45.24.39

Taking advantage of XRD patterns, the experimental lattice parameter a(Å) calculated at the (311) peak at different temperatures and concentration for Al, with the following relationship [11]:

$$a = d\sqrt{h^2 + k^2 + l^2} \text{..... (1)}$$

Where d is the interplanar spacing,and (h, k, and l) are the Miller indices The average crystal sizes (D) of Ni-Zn Ferrites are calculated by determining the angular location (2θ) and the peak width (FWHM) of the (311) peak using the Debye-Scherer equation [12]:

$$D = \frac{k\,\lambda}{\beta\,cos\theta} \text{..... (2)}$$

Where λ is X-Ray wave length of Cu–Kα radiation (0.15406 nm), K is Scherrer factor (0.9), β is full with at half maxima (FWHM), and θ is Bragg's diffraction angle. The jump lengths of the ions in the tetrahedral L_A and octahedral L_B, was calculated by the following relationships [13]:

LA=0.25a√3…… (3)

LB=0.25a√2…..... (4)
the theoretical density values ($\rho_{x\text{-}ray}$) of the Al-Ni-Zn Ferrite compound were calculated at different temperatures (400°C, 600°C, 800°C) with varying Al content (x = 0.0 to 0.5) was calculated using the following relationship [14]:

ρ x= 8M/Na3 ……. (5)

Where "M" is the molecular weight of the prepared ferrite, "N" is Avogadro's constant. Table 1 shows the calculated values for the crystal lattice constant (a), average crystal sizes (D), jump lengths (L_A, L_B), and theoretical density values ($\rho_{x\text{-}ray}$) of Ni0.5Zn0.5AlxFe2-xO4 at temperatures (as burned, 400°C, 600°C, and 800°C) and (x = 0.00 to 0.50 in 0.05 increments).

Table 1 XRD calculations of Ni-Zn-Al ferrite nanoparticles with varying Al content (x = 0.0 to 0.5) calcined at different temperatures

Sample	T (°C)	2Theta	FWHM	D(nm)	d (Å)	a (Å)	ρ (g/cm^3)	L_A(Å)	L_B(Å)
X=0.0	As-burnt	35.52	0.54	15.33	2.526	8.377	5.372	3.6272	2.9616
	400	35.54	0.57	14.64	2.524	8.371	5.383	3.6247	2.9596
	600	35.52	0.51	16.36	2.525	8.376	5.374	3.6267	2.9612
	800	35.47	0.5	16.68	2.529	8.386	5.353	3.6314	2.9650
X=0.05	400	35.55	0.52	16.04	2.523	8.368	5.356	3.6234	2.9585
	600	35.54	0.5	16.68	2.524	8.371	5.35	3.6247	2.9596
	800	35.52	0.44	18.96	2.526	8.376	5.340	3.6271	2.9615

Journal of Media, Culture and Communication
ISSN: 2799-1245
Vol: 04, No. 05, Aug-Sep 2024
http://journal.hmjournals.com/index.php/JMCC
DOI: https://doi.org/10.55529/jmcc.45.24.39

X=0.1	400	35.57	0.46	18.14	2.522	8.365	5.329	3.6221	2.9574
	600	35.56	0.49	17.03	2.523	8.366	5.326	3.6228	2.958
	800	35.54	0.43	19.40	2.524	8.371	5.318	3.6247	2.9596
X=0.15	400	35.57	0.45	18.54	2.522	8.363	5.299	3.6215	2.9569
	600	35.58	0.48	17.38	2.521	8.362	5.302	3.6208	2.9564
	800	35.62	0.38	21.96	2.518	8.353	5.319	3.6169	2.9532
X=0.2	400	35.62	0.43	19.41	2.519	8.353	5.286	3.6170	2.9532
	600	35.6	0.47	17.75	2.52	8.357	5.278	3.6188	2.9548
	800	35.63	0.35	23.84	2.518	8.351	5.291	3.6159	2.9524
X=0.25	400	35.63	0.42	19.87	2.518	8.351	5.256	3.6163	2.9527
	600	35.62	0.46	18.14	2.518	8.353	5.254	3.6169	2.9532
	800	35.67	0.32	26.08	2.515	8.341	5.275	3.6120	2.9492
X=0.3	400	35.64	0.42	19.87	2.517	8.349	5.228	3.6151	2.9517
	600	35.65	0.45	18.54	2.516	8.346	5.234	3.6139	2.9508
	800	35.72	0.29	28.78	2.512	8.330	5.263	3.6071	2.9452
X=0.35	400	35.67	0.39	21.40	2.515	8.342	5.209	3.6121	2.9492
	600	35.68	0.445	18.75	2.514	8.339	5.213	3.611	2.9484
	800	35.73	0.29	28.78	2.511	8.329	5.233	3.6065	2.9447
X=0.4	400	35.67	0.38	21.96	2.515	8.342	5.175	3.6123	2.9494
	600	35.72	0.43	19.41	2.512	8.33	5.197	3.6071	2.9452
	800	35.75	0.28	29.81	2.510	8.323	5.210	3.6041	2.9428
X=0.45	400	35.72	0.34	24.55	2.512	8.331	5.162	3.6076	2.9456
	600	35.75	0.42	19.87	2.510	8.323	5.177	3.6041	2.9428
	800	35.76	0.25	33.39	2.509	8.321	5.182	3.6030	2.9418
X=0.5	400	35.72	0.33	25.29	2.512	8.330	5.132	3.6069	2.9450
	600	35.78	0.42	19.88	2.508	8.317	5.156	3.6012	2.9404
	800	35.80	0.21	39.75	2.506	8.312	5.165	3.5992	2.9387

Structural Characterization

Lattice Parameter (a)

Fig. 2 shows that the values of lattice parameters for Al-Ni-Zn Ferrite calculated from relationship 1 decrease with increasing Al content as shown in Table 1. The difference in ionic radii between iron and aluminum explains this drop in the lattice constant. The Fe^{3+} ion has an ionic radius of 0.67 Å, whereas the Al^{3+} ion has an ionic radius of 0.51 Å [15]. The variation of the lattice constant is mainly related to the temperature variation. As the value of the lattice constant increases with increasing temperature when the aluminum content (x) is fixed due to differences in microstructure and surface defects, this can be explained by the fact that the ions move more quickly at higher temperatures, which leads to the expansion of the crystal lattice. However, the lattice constant begins to decrease with a further increase in temperature when the aluminum concentration increases. This trend may result from the sintering process, in which greater temperatures encourage densification and grain formation, which lowers the lattice parameter as a result of better crystal structure and fewer lattice defects. Literature has also found similar results for the crystal lattice constant of Al-Ni-Zn Ferrite. [16]

Journal of Media, Culture and Communication
ISSN: 2799-1245
Vol: 04, No. 05, Aug-Sep 2024
http://journal.hmjournals.com/index.php/JMCC
DOI: https://doi.org/10.55529/jmcc.45.24.39

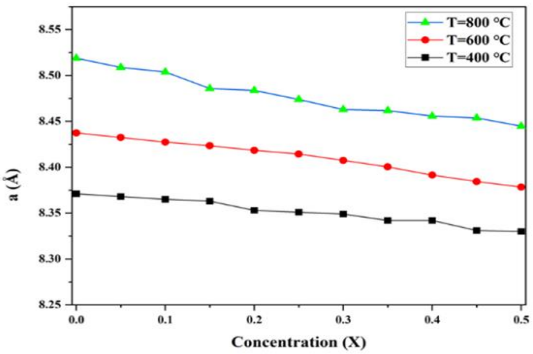

Fig.2 the variation of the lattice constant with Aluminum Content (x) for Ni-Zn ferrites at different calcination temperatures (400°C, 600°C, 800°C)

Crystallite Size (D)

Using X-ray diffraction (XRD) analysis, the Scherer equation (Equation 2) was used to calculate the crystallite size (D) by determining the angular position (2θ) and peak width (FWHM) of the (311) peak. The particle sizes of the particle size of Ni0.5Zn0.5AlxFe2-xO4 for all samples is within the nanoscale in range (14.64-39.75nm), as shown in Table 1. Fig. 3 shows the crystalline size grows quickly with increasing calcination temperature at fixed concentration of, and increases mainly with increasing aluminum content when the calcination temperature is constant. This rise is caused by the variance in the cation radii [17]. Previous studies have shown that large crystals were produced by raising the calcination temperature and aluminum content [18].

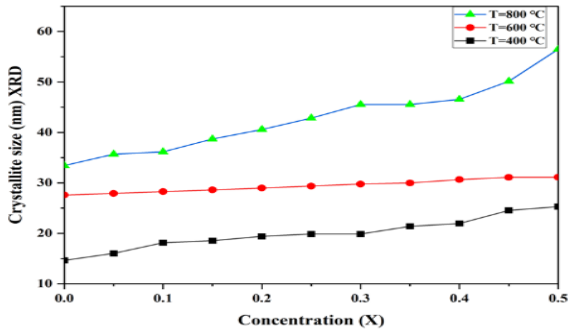

Fig. 3 Change in Crystallite Size with Aluminum Content (x) for Ni-Zn Ferrites at various Calcination Temperatures (400°C, 600°C, 800°C)

Theoretical Density (ρx-ray)

Theoretical Density ρx was calculated from relation 5 for Ni0.5Zn0.5AlxFe2-xO4 as shown in Table 1. Fig. 4 shows the decreases in the density with the increases of aluminum content. This change in behavior is a result of the different molar masses of iron (Fe^{3+}) and aluminum (Al^{3+}), which are 26.98 and 55.85 g/mol, respectively. Because aluminum has a lower atomic weight than iron, substituting Al^{3+} with Fe^{3+} reduces density, a result that is observed at all temperatures [19]. It is noted that the density decreases at Al content ($x \geq 0.1$) with increasing temperature, when Al content increases to ($x \geq 0.15$), the density begins to rise with increasing temperature. This behavior can be explained by several factors related to each other, as when the iron ion (Fe^{3+}) is replaced by an aluminum ion (Al^{3+}), the size of the crystal unit shrinks

Journal of Media, Culture and Communication
ISSN: 2799-1245
Vol: 04, No. 05, Aug-Sep 2024
http://journal.hmjournals.com/index.php/JMCC
DOI: https://doi.org/10.55529/jmcc.45.24.39

because the aluminum ion is smaller in size. This results to improved crystal structure at high temperatures, where density is increased by reducing crystalline defects and internal voids through having a more regular structure. Additionally, it also, high temperature increases the efficiency of sintering processes, grain cohesion, reduces gaps, and increases density. Including, at low aluminum levels ($X \geq 0.1$), irregular distribution of ions can lead to low density, but when aluminum content increases ($X \geq 0.15$) the ionic distribution in the crystal structure improves, increasing the density at high. Similar results can be found in the literature for doped ferrite with different sizes [19].

Fig. 4 shows the variation of the lattice constant with Aluminum Content (x) for Ni-Zn ferrites at different calcination temperatures (400°C, 600°C, 800°C)

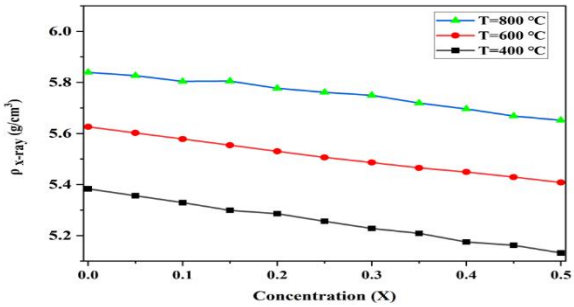

Hopping Length (L)

The distance between the magnetic ions, was calculated based on the crystal lattice constant using equations 3 and 4 respectively, for the prepared Ni-Zn ferrites samples. Figures 5 shown that the ionic jump lengths decrease with increasing Al content, Because Al ions are smaller than Fe ions, their substitution causes the lattice parameter to decreases, resulting in a more compact crystal structure [20] .The ionic jump lengths (LA and LB) are directly proportional to the value of the lattice constant (a) resulting in a decrease in the ionic jump lengths with increasing Al concentration. The ionic jump length LB is slightly smaller than LA because the LB sites are more compact and restricted. Compared to LA locations, resulting in shorter jumping distances [16].

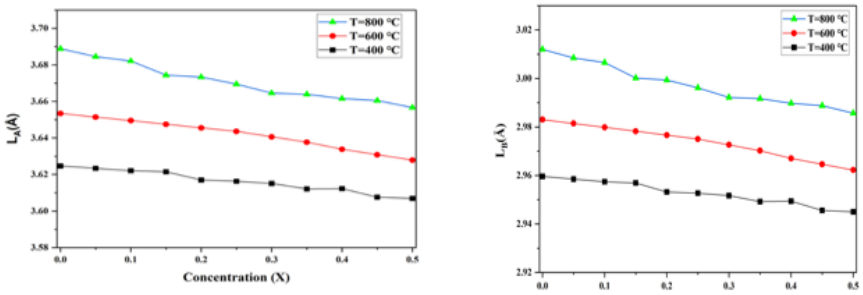

Fig. 5 shows the temperature variation with the jump length (a) L_A , and (b) L_B for a nanocomposite ferrite with the formula ($Ni_{0.5}Zn_{0.5}Al_xFe_{2-x}O_4$) at concentrations (X=0 - 0.5)

Fourier Transform Infrared (FT-IR) Spectroscopy

Journal of Media, Culture and Communication
ISSN: 2799-1245
Vol: 04, No. 05, Aug-Sep 2024
http://journal.hmjournals.com/index.php/JMCC
DOI: https://doi.org/10.55529/jmcc.45.24.39

Infrared spectroscopy is used to obtain a detailed analysis of cation distribution and structural distortions in spinel-structured for $Ni_{0.5}Zn_{0.5}Al_xFe_{2-x}O_4$ ferrites. The FTIR spectra between the ranges of 400 - 4000 cm^{-1} are displayed in Fig. 6, indicating many absorption bands that correspond to various vibrational modes due to specific chemical bonds and functional groups in the material investigated. As shown in Table 2, two main absorption bands ranges occur within the region of 400 to 800 cm^{-1} (bands v_1 &v_2). Band v_1 (530 to 550 cm^{-1}): this band is due to the stretching vibrations of metal-oxygen bonds ($M_{tetra} \leftrightarrow O$) (stretching vibrations of metal ions) in tetrahedral (A) sites. It represents the character and the strength of M-O bonds in tetrahedral sites. While band v_2 (400 to 420 cm^{-1}): is refer to the stretching vibrations of metal-oxygen bonds ($M_{octa} \leftrightarrow O$) (stretching vibrations of metal ions) in octahedral (B) sites, which reflects properties of M-O bonds in octahedral sites [21]. The v_1 band shifts from 533.045 cm^{-1} to 550.580 cm^{-1} with increasing Al content and calcination temperature; on its part, the v_2 band shifts from 406.866cm^{-1} to 421.144cm^{-1}. These shifts are an indication that there has been a reduction in bond lengths both in tetrahedron and octahedron sites as a result of substitution of smaller sized Al^{3+} ions for Fe^{3+} ions coupled with enhanced cation ordering and reduced structural distortions upon heating [22] .The FTIR spectra show additional absorption bands between 1400 and 3600 cm^{-1} for the prepared compounds. These bands correspond to nitrate ions (NO_3^-), carbon dioxide (CO_2) stretching frequencies, and the bending vibrations of water molecules, either absorbed or free (O-H). This is shown in figures 4.6-4.10. The high temperature during the combustion process reduces the intensity of carboxyl, hydroxyl, and nitrate groups, as noted in earlier studies [23].

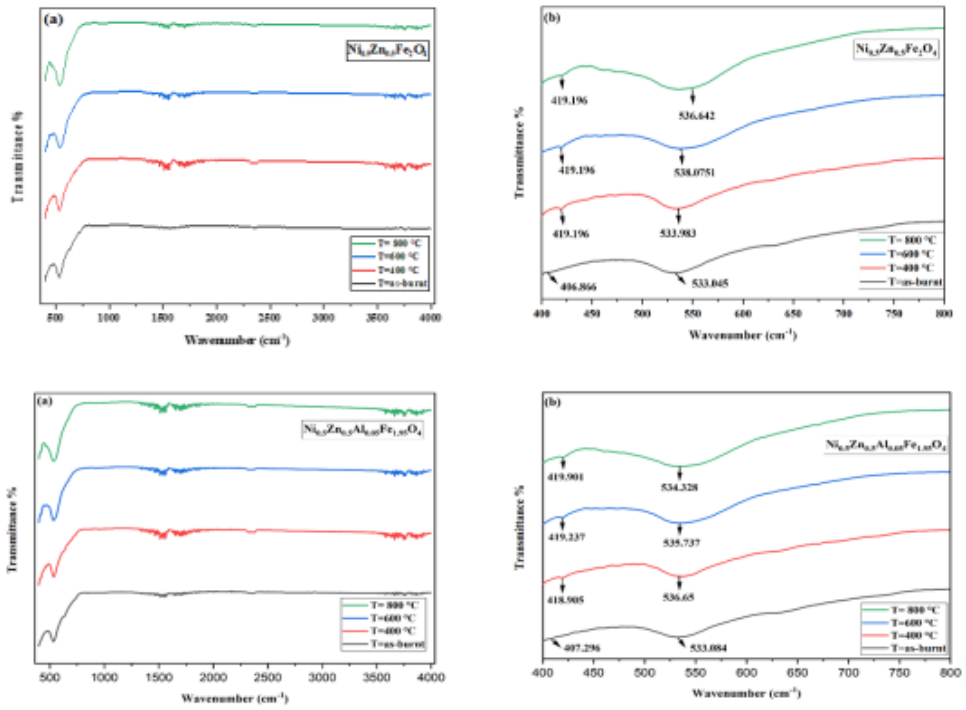

Journal of Media, Culture and Communication
ISSN: 2799-1245
Vol: 04, No. 05, Aug-Sep 2024
http://journal.hmjournals.com/index.php/JMCC
DOI: https://doi.org/10.55529/jmcc.45.24.39

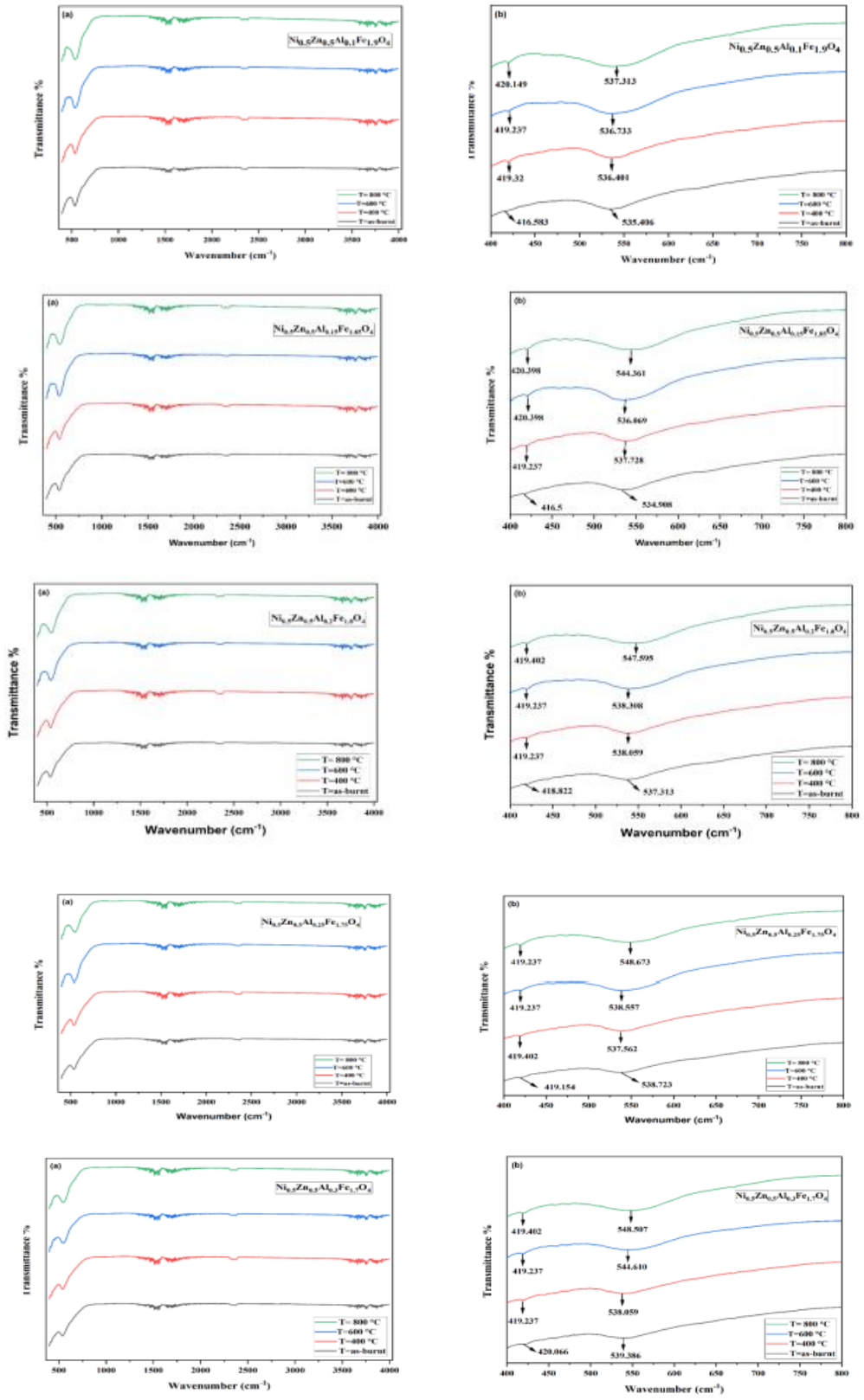

Journal of Media, Culture and Communication
ISSN: 2799-1245
Vol: 04, No. 05, Aug-Sep 2024
http://journal.hmjournals.com/index.php/JMCC
DOI: https://doi.org/10.55529/jmcc.45.24.39

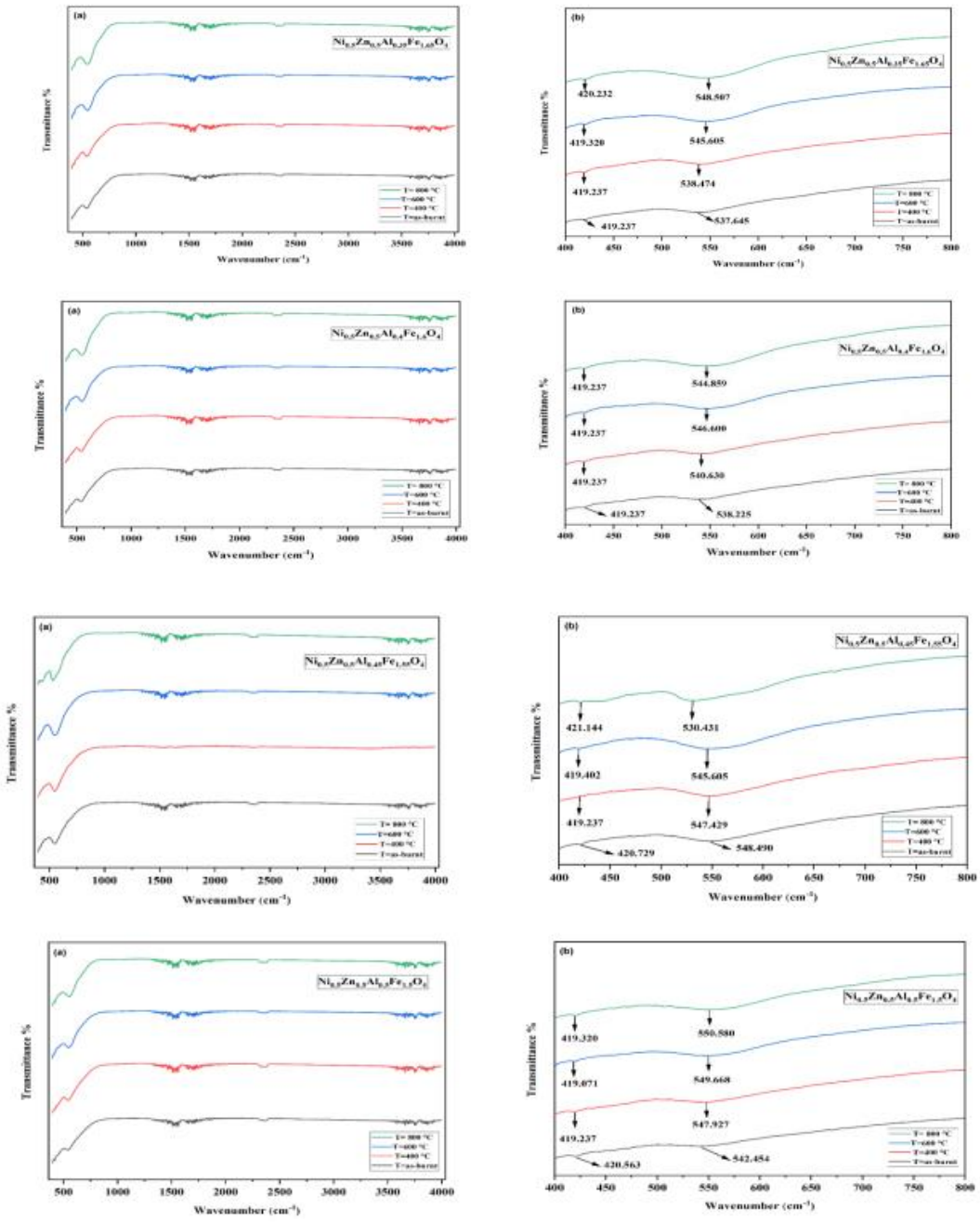

Fig. 6 FTIR Vibrational Patterns of Ni-Zn Ferrites with Aluminum Doping Level x =(0 - 0.5), Calcined at Different Temperatures (as burnt, 400°C, 600°C, and 800°C) in the Following Wavenumber Ranges: (a) 400 cm^{-1} to 4000 cm^{-1}; (b) 400 cm^{-1} to 800 cm^{-1}.

Table 2 FTIR Analysis of Al-Ni-Zn Ferrite Nanoparticles with Varying Al Content (x = 0.0 to 0.5) Calcined at Different Temperatures (as burnt, 400°C, 600°C, and 800°C).

X(mol)	T (°C)	V2	V1
	As-burnt	406.866	533.045

Journal of Media, Culture and Communication
ISSN: 2799-1245
Vol: 04, No. 05, Aug-Sep 2024
http://journal.hmjournals.com/index.php/JMCC
DOI: https://doi.org/10.55529/jmcc.45.24.39

X=0	400	419.196	533.983
	600	419.196	538.075
	800	419.196	536.642
X=0.1	As-burnt	416.583	535.406
	400	419.32	536.401
	600	419.237	536.733
	800	420.149	537.313
X=0.2	As-burnt	418.822	537.313
	400	419.237	538.059
	600	419.237	538.308
	800	419.402	547.595
X=0.3	As-burnt	420.066	539.386
	400	419.237	538.059
	600	419.237	544.610
	800	419.402	548.507
X=0.4	As-burnt	419.237	538.225
	400	419.237	540.630
	600	419.237	546.600
	800	419.237	544.859
X=0.5	As-burnt	420.563	542.454
	400	419.237	547.927
	600	419.071	549.668
	800	419.320	550.580
X=0.05	As-burnt	407.296	533.084
	400	418.905	536.65
	600	419.237	535.737
	800	419.901	534.328
X=0.15	As-burnt	416.5	534.908
	400	419.237	537.728
	600	420.398	536.069
	800	420.398	544.361
X=0.25	As-burnt	419.154	538.723
	400	419.402	537.562
	600	419.237	538.557
	800	419.237	548.673
X=0.35	As-burnt	419.237	537.645
	400	419.237	538.474
	600	419.320	545.605
	800	420.232	548.507
X=0.45	As-burnt	420.729	548.490
	400	419.237	547.429
	600	291.402	545.605
	800	421.144	530.431

Journal of Media, Culture and Communication
ISSN: 2799-1245
Vol: 04, No. 05, Aug-Sep 2024
http://journal.hmjournals.com/index.php/JMCC
DOI: https://doi.org/10.55529/jmcc.45.24.39

5. CONCLUSIONS

Nanopowder of Ni0.5Zn0.5AlxFe2-xO4 (x = 0.00 to 0.50 in 0.05 increments) was obtained by the sol-gel spontaneous combustion method, and calcined at temperatures of 400, 600, and 800 for three hours. Structural characterization was performed based on XRD and FTIR analysis. The XRD patterns show that the ferrite phase appears clearly, and the intensity of the peaks increases with increasing temperature, and that the greatest intensity appears at the peak (311) for all samples, and it becomes clearer with increasing calcination temperature. The parameters of the crystal structure of the ferrite prepared from the XRD patterns were studied. The results showed the following: The values of the lattice constant a for Al-Ni-Zn ferrite decrease with increasing Al content, and this is due to the difference in the ionic radius between the iron and the aluminum substituted within the ferrite matrix. The value of the lattice constant a also increases with increasing temperature, as high temperatures cause densification and grain formation, which results in a better crystalline structure and fewer lattice defects. The crystal size D increases with increasing calcination temperature and with increasing aluminum content due to the variation in the radius of the cations. A decrease in density (ρx-ray) appears with increasing aluminum content due to the difference in molar masses of iron (Fe^{3+}) and aluminum (Al^{3+}). The density at Al ($x \geq 0.1$) also decreases with increasing temperature, and increases at ($x \geq 0.15$), due to the shrinkage of the size of the crystal unit because the aluminum ion is smaller in size. The ion jump lengths decrease with increasing Al content. Because Al ions are smaller than Fe ions, their substitution results in a lower lattice parameter, resulting in a more compact crystal structure. Infrared spectroscopy revealed two main absorption bands: Band v1 (530 to 550 cm^{-1}): This band is due to the metal-oxygen bond stretching vibrations in the tetrahedral sites (A). Band v2 (400 to 420 cm^{-1}): refers to the metal-oxygen bond stretching vibrations in the octahedral sites (B). A shift towards higher values occurs because there is a decrease in bond lengths in both the tetrahedral and octahedral sites as a result of the substitution of smaller Al^{3+} ions by Fe^{3+} ions.

6. REFERENCES

1. Verma, A., Goel, T. C., Mendiratta, R. G., & Gupta, R. G. (1999). High-resistivity nickel–zinc ferrites by the citrate precursor method. Journal of magnetism and magnetic materials, 192(2), 271-276.
2. Yue, Z., Zhou, J., Li, L., & Gui, Z. (2001). Effects of MnO2 on the electromagnetic properties of NiCuZn ferrites prepared by sol-gel auto-combustion. Journal of magnetism and magnetic materials, 233(3), 224-229.
3. Chen, D. G., Tang, X. G., Wu, J. B., Zhang, W., Liu, Q. X., & Jiang, Y. P. (2011). Effect of grain size on the magnetic properties of superparamagnetic Ni0. 5Zn0. 5Fe2O4 nanoparticles by co-precipitation process. Journal of Magnetism and Magnetic Material.
4. Zahi, S., Hashim, M., & Daud, A. R. (2007). Synthesis, magnetic properties and microstructure of Ni–Zn ferrite by sol–gel technique. Journal of Magnetism and Magnetic Materials, 308(2), 177-182.

Journal of Media, Culture and Communication
ISSN: 2799-1245
Vol: 04, No. 05, Aug-Sep 2024
http://journal.hmjournals.com/index.php/JMCC
DOI: https://doi.org/10.55529/jmcc.45.24.39

5. Kumar, K. V., Paramesh, D., & Reddy, P. V. (2015). Effect of aluminium doping on structural and magnetic properties of Ni-Zn ferrite nanoparticles. World Journal of Nano Science and Engineering, 5(03), 68.
6. Shahane, G. S., Kumar, A., Arora, M., Pant, R. P., & Lal, K. (2010). Synthesis and characterization of Ni–Zn ferrite nanoparticles. Journal of Magnetism and Magnetic Materials, 322(8), 1015-1019.
7. Jahan, N., Khan, M. N. I., Hasan, M. R., Bashar, M. S., Islam, A., Alam, M. K., ... & Khandaker, J. I. (2022). Correlation among the structural, electric and magnetic properties of Al 3+ substituted Ni–Zn–Co ferrites. RSC advances, 12(24), 15167-15179.
8. Zuhroh, S., Hidayah, A. S. N., Aturroifah, N. I. M., Wahyuni, N. E. A., & Utomo, J. (2022, June). Study of Phase Transformation, Structures, Morphology, and Vibration of Ni-Zn-Co Ferrites Nanoparticles due to Annealing Temperature. In Journal of Physics: Conference Series (Vol. 2243, No. 1, p. 012051). IOP Publishing.
9. Yadav, Raghvendra Singh, et al. "Anneal-tuned structural, dielectric and electrical properties of ZnFe 2 O 4 nanoparticles synthesized by starch-assisted sol–gel auto-combustion method." Journal of Materials Science: Materials in Electronics 27 (2016): 59.
10. Mahalakshmi, S., SrinivasaManja, K., & Nithiyanantham, S. (2014). Electrical properties of nanophase ferrites doped with rare earth ions. Journal of Superconductivity and Novel Magnetism, 27, 2083-2088.
11. Ridha, Sabah M. Ali, and Aveen Areef Ali. "Effect of heat treatments on the structural and magnetic properties of nickel ferrite nanopowders prepared using the sol-gel autocombustion technique." NeuroQuantology 20.7 (2022): 2329.
12. Ridha, Sabah M. Ali, and Hussam A. Khader. "XRD and SEM characteristics of Co-Ni ferrite nanoparticles Synthesized using sol-gel method." Turkish Journal of Computer and Mathematics Education (TURCOMAT) 12.14 (2021): 675-687.
13. Gandhad, Sheela S., et al. "Structural, Williamson-Hall Plot and Size-strain Analysis of MgxNi1-xAlxFe2-xO4 Ferrites." Int. J. Adv. Sci. Eng 5.4 (2019): 1146-1153.
14. Mohammad, Ali M., Sabah M. Ali Ridha, and Tahseen H. Mubarak. "Dielectric properties of Cr-substituted cobalt ferrite nanoparticles synthesis by citrate-gel auto combustion method." Int. J. Appl. Eng. Res 13.8 (2018): 6026-6035.
15. Srivastava, M., Chaubey, S., & Ojha, A. K. (2009). Investigation on size dependent structural and magnetic behavior of nickel ferrite nanoparticles prepared by sol–gel and hydrothermal methods. Materials Chemistry and Physics, 118(1), 174-180.
16. Rafferty, A., Gun'ko, Y., & Raghavendra, R. (2009). An investigation of co-fired varistor-NiZn ferrite multilayers. Materials Research Bulletin, 44(4), 747-752.
17. Javed Iqbal, M., Ahmad, Z., Meydan, T., & Melikhov, Y. (2012). Physical, electrical and magnetic properties of nano-sized Co-Cr substituted magnesium ferrites. Journal of applied physics, 111(3).
18. Yan, Wenxun, et al. "Characterization and low-temperature sintering of Ni0. 5Zn0. 5Fe2O4 nano-powders prepared by refluxing method." Powder Technology 192.1 (2009): 23-26.
19. Zenger, M. (1994). Modern ferrite technologies and products. International Journal of Materials and Product Technology, 9(4-6), 265-280.

Journal of Media, Culture and Communication
ISSN: 2799-1245
Vol: 04, No. 05, Aug-Sep 2024
http://journal.hmjournals.com/index.php/JMCC
DOI: https://doi.org/10.55529/jmcc.45.24.39

20. Yan, W., Li, Q., Zhong, H., & Zhong, Z. (2009). Characterization and low-temperature sintering of Ni0. 5Zn0. 5Fe2O4 nano-powders prepared by refluxing method. Powder Technology, 192(1), 23-26.
21. Zhang, M., Zi, Z., Liu, Q., Zhang, P., Tang, X., Yang, J., ... & Dai, J. (2013). Size effects on magnetic properties of Ni0. 5Zn0. 5Fe2O4 prepared by sol-gel method. Advances in Materials Science and Engineering, 2013(1), 609819.
22. Roy, P. K., & Bera, J. (2007). Enhancement of the magnetic properties of Ni–Cu–Zn ferrites with the substitution of a small fraction of lanthanum for iron. Materials research bulletin, 42(1), 77-83.
23. Joseyphus, R. J., Narayanasamy, A., Jeyadevan, B., Shinoda, K., & Tohji, K. (2006, May). Superparamagnetic Particle Size Limit of Mn-Zn Ferrite Nanoparticles Synthesised Through Aqueous Method. In AIP Conference Proceedings (Vol. 833, No. 1, pp. 31-34). A.